Investigating Additive Manufactured Lattice Structures: A Multi-Instrument Approach

(Article begins on next page)

This article has been accepted for publication in a future issue of this journal, but has not been fully edited. Content may change prior to final publication. Citation information: DOI 10.1109/TIM.2019.2959293, IEEE Transactions on Instrumentation and Measurement

Investigating additive manufactured lattice structures: a multi-instrument approach

Gloria Allevi, Lorenzo Capponi, Paolo Castellini, Paolo Chiariotti, Franco Docchio, Fabrizio Freni, Roberto Marsili, Milena Martarelli, Roberto Montanini, Simone Pasinetti, Antonino Quattrocchi, Robert Rossetti, Gianluca Rossi, Giovanna Sansoni, Enrico Primo Tomasini

Abstract— **Additive manufacturing (AM) is gaining relevance for the freedom it gives to designers in experimenting topologically optimized components, especially those having lattice morphology. Indeed, these are of great interest in various application fields (automotive, biomedical, etc.) because, in addition to a significant mass reduction, lattice topology (micro-scale) can be tuned to provide the final product (macro-scale) with the specific properties it needs to exhibit. However, additive manufactured lattice structures are still to be fully investigated, given the mismatch between the designed and the manufactured final product.**

This paper presents some preliminary results from a multi-instrument approach, grounding on non-contact measurement techniques, to characterize lattice and trabecular structures in terms of dimensional accuracy, surface morphology, stress-strain distribution and modal behavior.

Index Terms— **additive manufacturing (AM), lattice structures, 2D vision systems, digital image correlation, thermoelastic stress analysis, laser Doppler vibrometry**

I. Introduction

Additive Manufacturing (AM) has gained disruptive relevance in engineering applications for the high flexibility achievable in terms of design: geometrically complex shapes [1, 2, 3, 4] are reproduced without the typical constraints of shaving removal. Among the possible structures, those presenting lattice/trabecular morphology are becoming standard in various fields, from automotive to biomedical. In fact, lattice/trabecular morphology gives the possibility to optimize topology of a structure, thus achieving important mass reduction and improved characteristic properties of the structure itself, like fine-tuned stiffness or improved thermal properties. However, despite the clear advantages of 3D printing technology, the structural response of 3D printed lattice components can be significantly different, from the designed one, no matter the material adopted. This enforces the necessity to experimentally identify dissimilarities to better understand both 3D printing mechanism associated to these structures and better control the design/production process to provide higher reliability to the final product. This is a complex task, which necessarily requires a multi-instrumental and multi-competence approach.

The few studies [5] already published on this topic prove the necessity to analyse more in-depth the mechanical behaviour of trabecular structures. While finite elements numerical analyses [6, 7] have been performed, experimental characterization has been limited to stress-strain curves estimation by compression tests, to porosity evaluation through electron scanning microscopy [8] and to investigation of materials crystalline structure composition by electronic backscatter diffraction [9]. In the end, there are few examples of non-invasive characterization of these structures and the target is mainly validation of numerical models [6, 10, 11, 12, 13, 14].

Contrarily, the aim of the present paper is to develop proper experimental protocols based on advanced non-contact measurement techniques to qualify lattice structures. For this reason, different techniques, such as 2D vision systems, digital image correlation (DIC), thermo-elastic stress analysis (TSA) and laser Doppler vibrometry, have been used to assess dimensional stability and surface characteristics, to map global and local stress-strain fields, and to analyse the modal behaviour of simple structures with lattice morphology.

The paper, which is an extended version of the one presented at the recent IEEE I²MTC 2019 [15], is organized as follows: the specimens investigated, and the experimental techniques adopted are presented in Section II; Section III discusses the main results of the analyses performed; Section IV draws the conclusions of the activity.

II. Material and Methods

A. Elementary trabecular samples

Fig. 1 shows the three samples used in the study. The first specimen (Fig. 1 a) has a square elementary cell of 3 × 3 mm

P. Castellini, P. Chiariotti, M. Martarelli, Robert Rossetti and E.P. Tomasini are with the Department of Industrial Engineering and Mathematical Sciences, Università Politecnica delle Marche, Ancona, 60131 Italy (e-mails: p.castellini@univpm.it, p.chiariotti@univpm.it, m.martarelli@univpm.it, r.rossetti@univpm.it, ep.tomasini@univpm.it)

Gloria Allevi and Lorenzo Capponi are with CISAS "G. Colombo", Università degli Studi di Padova, Padova, 35122 Italy (e-mail: gloria.allevi@phd.unipd.it, lorenzo.capponi@phd.unipd.it).

Franco Docchio, Simone Pasinetti, Giovanna Sansoni are with Department of Mechanical and Industrial Engineering, Università degli Studi di Brescia, 25123 Italy (e-mails: franco.docchio@unibs.it, simone.pasinetti@unibs.it, giovanna.sansoni@unibs.it)

Roberto Marsili and Gianluca Rossi are with Department of Engineering, Università degli Studi di Perugia, 06125 Italy (e-mails: roberto.marsili@unipg.it, gianluca.rossi@unipg.it).

Roberto Montanini, Fabrizio Freni and Antonino Quattrocchi are with Department of Engineering, Università degli Studi di Messina, 98122 Italy (e-mails: roberto.montanini@unime.it, fabrizio.freni@unime.it, antonino.quattrocchi@unime.it).

This article has been accepted for publication in a future issue of this journal, but has not been fully edited. Content may change prior to final publication. Citation information: DOI 10.1109/TIM.2019.2959293, IEEE Transactions on Instrumentation and Measurement

with a trabecular width of 2 mm; the second one (Fig. 1 b) has a rhombic elementary cell with diagonals of 6 - 20 mm and trabecular width of 2 mm. Both these samples were produced in Ti6Al4V alloy and printed by Electron Beam Melting (EBM). Their sizes are 120 × 20 × 5 mm with the same cross section.

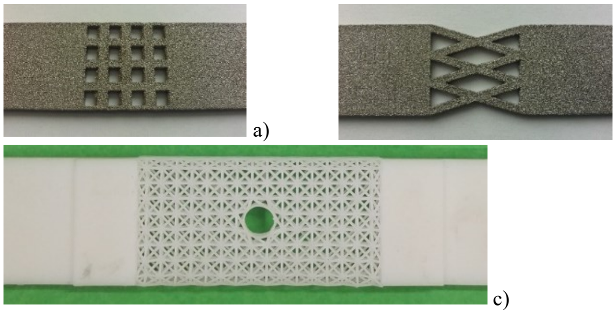

Fig. 1. Lattice samples with a) square, b) rhombic, C) cubic cell.

The third specimen (Fig. 1 c) has a finely detailed structure with a cubic cell of 3.50 mm that develops in the x, y and z directions. A hole of 5 mm of diameter was created in the middle of the sample. The sample sizes are 100 × 20 × 5mm. For its manufacturing, photopolymer resin (Clear FLGPCL03, Formlabs) and Stereolithography (SLA) were employed. All samples structures were chosen because they reproduce typical connections of lattice systems.

B. 2D vision systems setup

Machine vision was adopted to analyze the superficial geometry of the samples. Given the challenge provided by the third sample, the activity was carried on mainly on that specimen.

The test-bed is shown in Fig. 2. An IDS UI-1460SE CMOS camera was employed to analyze the lattice structure. The camera has a resolution of 2048 × 1536 pixels, a sensor size of ½" and was equipped with bi-telecentric lens (Opto Engineering TC23036 depth of field = 11 mm). The lattice structure was placed in front of the objective, on a rigid support. The structure was located at 102.5 mm from the objective. Two motorized linear stages, with ±0.1 µm resolution, were used to center the structure with respect to the field of view of the camera. The final field of view was 26.3 × 19.7 mm.

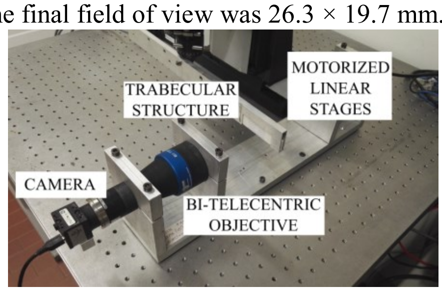

Fig. 2. 2D vision system test-bed.

Fig. 3 a) shows a sample image acquired with the camera. Image distortions and perspective errors were minimized by the adoption of the bi-telecentric lens. The structure was aligned with respect to the optical axis so that only the superficial layers of the structure were visible. Fig. 3 b) displays a zoomed part of a sector of the superficial layer of the structure. Each beam of the sector is correctly focused.

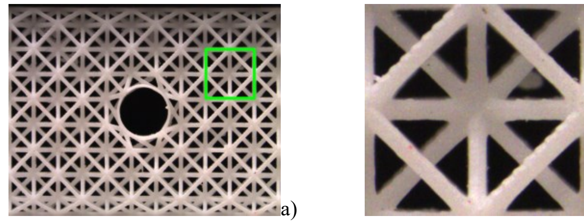

Fig. 3. Image acquired with the 2D vision system setup a). The green rectangle represents a single sector of the analyzed structure, zoomed in b).

The CAD model of the analyzed trabecular structure is shown in Fig. 4 a). The structure is superficially composed of a repetition of squared element, called sectors (Fig. 4 b)). The structure was dimensionally characterized analyzing each of these sectors and measuring the following four distances (Fig. 4 b)) by a specifically designed edge-detection-based algorithm:

- V, i.e. distance between vertical opposite vertices of the sector;
- O, i.e. distance between horizontal opposite vertices of the sector
- D_1, D_2, i.e. distances between opposite beams of the sector.

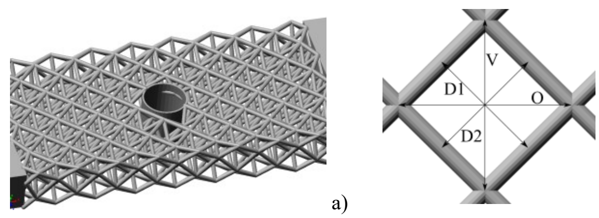

Fig.4. CAD model of the analyzed trabecular structure a), and of a single sector b).

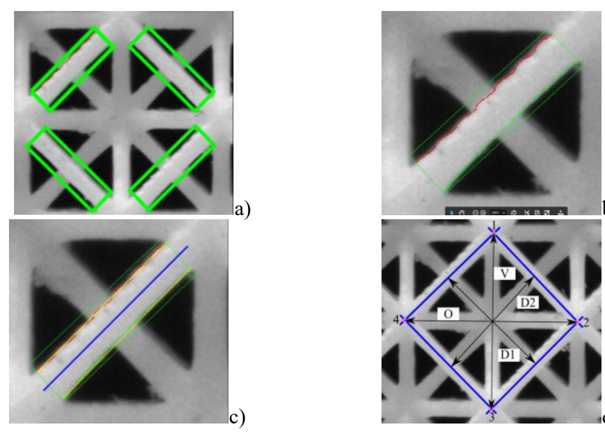

Fig. 5. Measurement algorithm using the 2D vision system setup. RoIs selection phase a), edges detection phase b), lines fitting phase c), and dimensional measurement phase d).

The measurements were performed following four different phases:

1. *RoIs selection* (Fig. 5 a)): four different rectangular Regions of Interest (RoI) were manually selected in the sector image. Each RoI was built around each beam of the sector.
2. *Edges detection* (Fig. 5 b)): a standard edge detection was performed in each RoI analyzing the gray levels of the pixels contained in the RoI. Left and right edges were split into two different groups (red and green points). The identified edges represent the limits of each beam.

This article has been accepted for publication in a future issue of this journal, but has not been fully edited. Content may change prior to final publication. Citation information: DOI 10.1109/TIM.2019.2959293, IEEE Transactions on Instrumentation and Measurement

3. *Lines fitting* (Fig. 5 c)): edges found in the previous phase were used to fit two straight lines on the beam edges (yellow segments). The beam axis was then detected computing the bisecting line of the yellow segments (blue segment).
4. *Dimensional measurements* (Fig. 5 d)): the final dimensional measurements were obtained considering the axes computed in each of the four RoIs.

C. Digital Image Correlation setup

DIC measurements were performed using a Canon EOS 7D camera, equipped with a hybrid image stabilizer and a 100 mm 1:2.8 L IS USM macro optic, and a commercial software (Limess DIC 2D) to cross-correlate images acquired. Specific tests were carried out to optimize the lighting conditions and the measuring parameters for extract the strain field. DIC was performed on the two metallic samples. As well as direct and diffused light, artificially created speckle and natural speckle provided by the rough surface of the samples were tested.

D. Thermal Stress Analysis setup

As for TSA measurements, an infrared camera (FLIR SC 7200) with InSb cooled sensor (320 × 256 pixels of resolution, NETD < 25 mK) and a dedicated image-processing software (Altair LI) were used. To increase robustness of results each specimen surface was painted whit a black opaque paint to homogenize its emissivity. Even though paint thickness homogeneity could not be guaranteed, different tests in preliminary phases showed that the emissivity homogeneity in the painted specimens was higher than in the non-painted ones, thus resulting in higher Signal to Noise Ratios. Tests were approached in two ways: globally framing the weft of interest, to evaluate the overall stress distribution on the structure and the interactions between the various weft portions, and locally using an IR close-up lens, able to focus the trabeculae in detail and to determine the surface stress state on the component.

E. Load system for DIC and TSA

A specifically designed loading system (Fig. 6) was adopted for DIC and TSA measurements. The system consists of a structure, two grips, one fixed and the other movable, four pneumatic cylinders and an electrodynamic shaker (LDS V650). The structure consists of four core columns, divided into three sections that join three metal plates. Threaded bars are located inside the columns. The lower and central plates have a hole for inserting a sliding bush within which the cylindrical bar moves. An extensometric load cell is screwed on the cylindrical bar head. The specimen is clamped at an end, while the other one is integral with the shaker sliding shaft. This last one, supplied by a power amplifier (LDS PA1000L) and a signal generator, is able to axially stress the sample. The four pneumatic pistons (FESTO DSNU-12-50-P-A) are used both to provide a preload (dynamic tests) and to apply a uniform load (static tests). The stress for the specimen is transmitted from the shaker head through a connecting rod with 2 spherical joints at the end. The structure is made of AISI 316 steel and has sufficient rigidity to guarantee the open loop use a frequency range from 0 to 500 Hz, while the structure lower portion presents an open loop operation limit relative to the first total system frequency of about 115 Hz. The whole solution provides a uniform load preventing formation of asymmetrical strains.

Fig. 6. Load system for DIC and TSA.

Fig. 7. Set-up for vibrational excitation by volume acoustic source

F. Experimental Modal Analysis setup

Laser Doppler Vibrometry (LDV) was adopted to characterize the dynamic behavior of the third specimen. Conventional excitation methods used in modal testing are effective for exciting global vibrational mode shapes, but they are not when it comes to exciting the single trabeculae. Two types of excitation were used: a non-contact acoustic excitation (it is well known that in lightweight structures non-contact methods should be preferred also in terms of excitation) for assessing the global mode shapes of the specimen and a piezo-based excitation to focus on the dynamics of trabeculae.

A mid-/high-frequency volume acoustic source (Fig. 7) placed 10 mm from the sample (tested in cantilever beam like configuration, so clamped at one end, free at the other) and driven with random signal in the range 0.2-10 kHz was used for assessing the global mode shapes of the specimen. The driving force is the acoustic strength of the monopole at the outlet of the source measured as volume acceleration. Given the non-punctual nature of the exciting system, torsional modes are barely excited. LDV measurements were performed on a 30 points grid (3 × 10 – 3 points on the short side of the specimen) over the whole target (the lattice and solid parts). A piezo-actuator (Fig. 8 a) was fixed to the specimen with epoxy glue. Two tests in different excitation ranges were performed: a first one in the 10-102 kHz range, and a second one in the 35-70 kHz range to reduce the influence of global modes. Given the characteristics of the piezoelectric and the installation mode, it was not possible to install a load cell to measure actual excitation force, to estimate the Frequency Response Function (FRF) and to obtain a reference signal. Given the impossibility to measure the force transmitted to the structure, the monitor signal provided by the power amplifier of the piezoelectric actuator was used as reference for Frequency Response Function (FRF) assessment (this means assuming a flat actuator response). The specimen was tested on a soft foam in free boundary conditions.

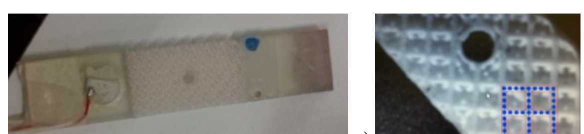

a) b)

Fig. 8. Piezo-based excitation set-up: piezo location a), investigation area on the trabeculae b).

The surface of the structure was coated with a very thin layer of lacquer: this strategy is targeted to improve the Signal to Noise

This article has been accepted for publication in a future issue of this journal, but has not been fully edited. Content may change prior to final publication. Citation information: DOI 10.1109/TIM.2019.2959293, IEEE Transactions on Instrumentation and Measurement

Ratio (SNR) of the vibration velocity measured by LDV. A grid of 45 points (Fig. 8 b), equally spaced and aligned with the superficial trabeculae, on a section of the structure in between the central hole and the solid part, was set as investigation grid.

III. RESULTS

A. 2D Vision system results

1) Metrological characterization of the experimental setups

The 2D vision system setup was characterized, at first, in terms of measurement reproducibility. A total of 50 measurements of distance D_2 were performed on a single sector of the trabecular structure. Measurements were obtained varying the measurement condition, i.e. modifying measurement parameters such as sector position (with respect to the field of view of the sensors), RoIs, etc. Results are reported in Table I.

TABLE I. RESULTS OF THE METROLOGICAL CHARACTERIZATION OF THE 2D VISION SYSTEM SETUP

	2D Vision system setup
Number of measurements	50
D_2 mean value [μm]	3449.8
D_2 standard deviation [μm]	3.5
Reproducibility (95%) [μm]	6.9

The setup shows good reproducibility with compatible measurements. The variability is probably due to the non-optimal alignment of the structure with respect to the optical axis of the imaging system.

2) Dimensional characterization of the trabecular structure

Each sector of the trabecular structure was dimensionally measured using the algorithm. Table II shows the measurement results in terms of measurement errors ε, defined as the difference between nominal and measured values. The latter term refers to measurements performed over all the exposed trabecular part of the specimen.

TABLE II. RESULTS OF THE DIMENSIONAL CHARACTERIZATION OF THE TRABECULAR STRUCTURE

Dimension (nominal value)	**2D Vision system setup**	
	Mean of ε [μm]	Standard deviation of ε [μm]
V (4950 μm)	98.3	33.7
O (4950 μm)	77.7	38.8
D_1 (3500 μm)	59.7	10.4
D_2 (3500 μm)	57.2	14.0

Results shows positive measurement errors, with maximum errors obtained for the dimension V. This means that the trabecular structure presents lower dimensions with respect to the nominal values. This can be due to plastic deformations due to the manufacturing process and to the material used to produce the structure. The variability of the dimensions of the sectors can be equally due to manufacturing process. This conclusion is confirmed analyzing the alignment of the structure in different areas along the field of view of the camera.

Fig. 9 shows details of two different zones of the structure. Zoom number 1 (top right part of the structure) shows good alignments since superior trabeculae hide inferior ones correctly. Zoom number 2 (bottom part of the structure) shows misalignments: lower trabeculae are not hidden by higher ones. This behavior is due to a plastic deformation of the structure.

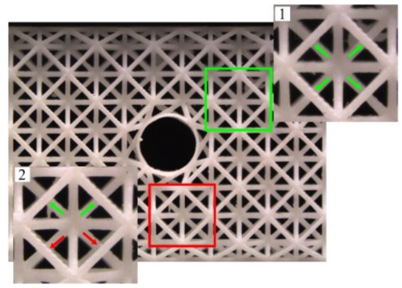

Fig. 9. Zoomed portions of two areas of the analyzed structure. Zoom n. 1 shows good alignment. Zoom n. 2 shows misalignments.

To further analyze the deformation, a tomographic scan of the structure was performed using an industrial equipment (NSI X5000, North Star Imaging) with 0.5 μm resolution. The tomographic scan and the CAD model were aligned using commercial software (Polyworks 2016, Innovmetric). Fig. 10 shows, in colormap form, deviation between the real structure and the nominal CAD model. The tomographic scan clearly shows the plastic deformation along the XZ plane of the structure. Focusing on the trabecular area of the structure, deviations up to 0.2 mm were obtained. The deviation identified is probably due to the standing surface chosen during the additive manufacturing process. If the structure had been made choosing other standing surfaces, plastic deformation would have spread toward other directions.

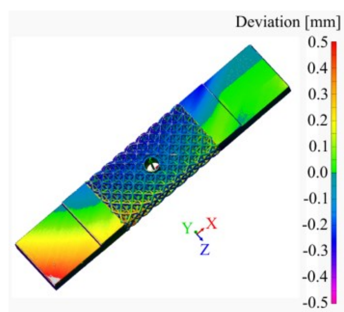

Fig. 10. Tomography of the analized structure. Colormap shows deviation between real structure and nominal CAD model.

Fig. 11 shows a section of the structure along the YZ plane. Black and red ellipses represent nominal and real trabeculae sections respectively. As expected, red ellipses have different dimensions and positions with respect to black ones. The difference between nominal and real sections increases toward structure edges.

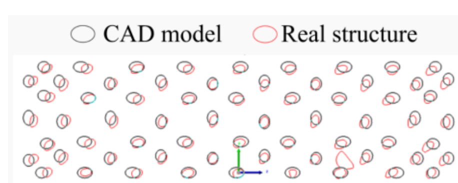

Fig. 11. Sample section of the analyzed structure along the YZ plane. Black and red ellipses represent nominal and real trabeculae sections respectively.

This article has been accepted for publication in a future issue of this journal, but has not been fully edited. Content may change prior to final publication. Citation information: DOI 10.1109/TIM.2019.2959293, IEEE Transactions on Instrumentation and Measurement

B. DIC results

To measure the strain state, static tensile tests were performed at the same load conditions for both the sample types, applying a variable load from 0 to 1000 N with a step of 250 N.

Fig. 12 shows the comparison between results obtained under direct and diffused lighting conditions on the samples with artificial speckle at a static traction load of 1000 N. Images well demonstrate importance of uniform lighting in the RoI. The best detail level is obtained in diffused lighting condition.

Fig. 13 shows the comparison between vertical displacement and strain field with natural speckle and diffused lighting under the most severe test conditions (load of 1000 N). Strain tends to focus on the minimum resistance sections. The strain asymmetry, between the crossings, is due to the screws non-homogeneous clamping.

C. TSA results

The TSA tests were designed to demonstrate the possibility of measuring the plane stress field of the elementary trabecular cells, without contact and with enough detail. Cyclical loads were performed, varying preload (from 20 to 200 N), peak-peak amplitude (from 30 to 250 N) and cycle frequency (from 10 to 70 Hz).

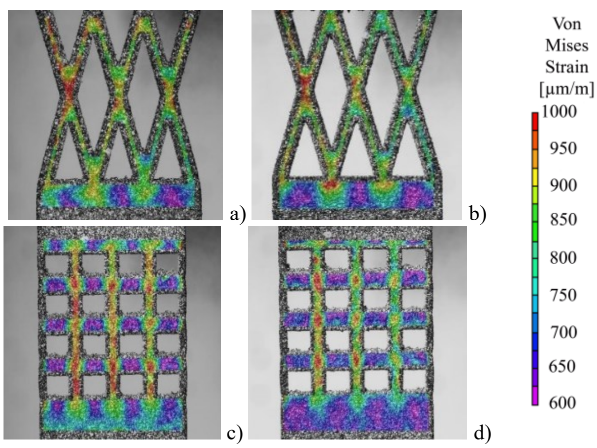

Fig. 12. Longitudinal strain full-field measurement, obtained by DIC: comparison between a), c) direct and b), d) diffuse lighting conditions on specimens with artificial speckle (F = 1000 N).

The tests were carried out in two ways. A 50 mm optic was used to totally focus the RoI and to evaluate the overall stress distribution on the structure. A 100X close-up lens was employed to analyze the individual interconnections between the various elementary specimen trabeculae and to allow a more detailed investigation of the surface stress field. Figs. 14 and 15 show the overall and detailed views. The thermoelastic signal is particularly high (stress tends to assume the highest values) at the trabeculae intersection areas for the rhombic weft specimen and along the vertical interconnections, parallel to the applied load direction, for the square weft specimen. The phase images highlight undesired edge effects presence due to rigid motions the sample was undergoing during the test. However, these effects can be compensated by dedicated images post-processing.

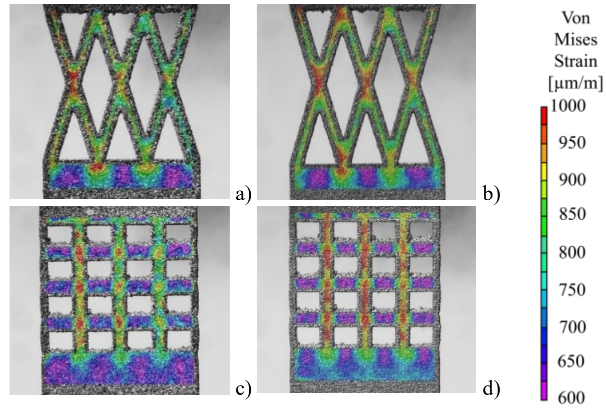

Fig.13.Longitudinal strain full-field measurement, obtained by DIC: comparison between diffused lighting conditions (F = 1000 N) with a), c) artificial and b), d) natural speckle.

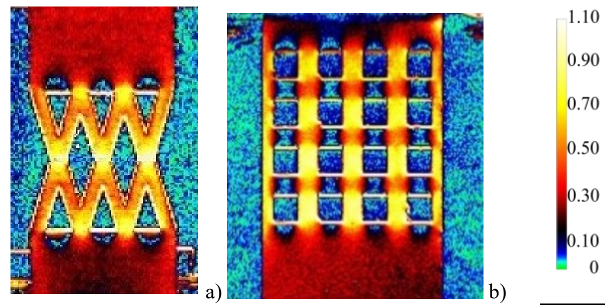

Fig. 14. Stress full-field measurement obtained by TSA, global study. Amplitude images obtained with preload of 200 N, peak-peak of 200 N, frequency of 50 Hz on trabecular specimen with a) rhombic and b) square elementary module.

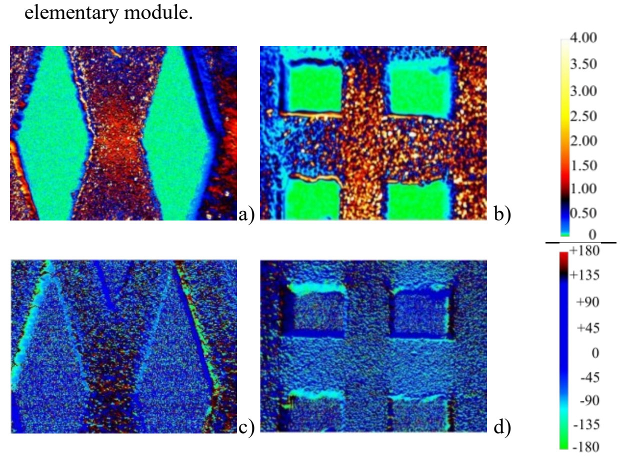

Fig.15.Stress full-field measurement obtained by TSA, local study with close-up optics. Amplitude images a), b) and phase c), d) obtained with preload of 200 N, peak-peak of 200 N, frequency of 50 Hz on trabecular specimen with elementary rhomboid (on the left) and square elementary module (on the right).

D. Finite Element Analysis (FEA) results

A FE simulation was also carried out using the commercial software ANSYS™ in order to compare strain results with those obtained experimentally (Fig. 16 and 17). The specimen geometries were obtained by directly importing the CAD models which had been used for printing them. The models were discretized using 1.5 mm shell elements, thickening the grid to 0.5 mm in the trabecular region. These discretization values made it possible to balance the goodness of results and computational effort. The printed material properties (Ti6Al4V

This article has been accepted for publication in a future issue of this journal, but has not been fully edited. Content may change prior to final publication. Citation information: DOI 10.1109/TIM.2019.2959293, IEEE Transactions on Instrumentation and Measurement

grade 5) were directly imported from the software database. The constraint and load conditions involve the presence of a lock at the upper edge and the application of a force of 1000 N at the lower one.

The numerical simulation shows good agreement with the experimental evidence. The most stressed regions, as already highlighted by the optical measurements, are concentrated at the trabeculae intersection for the rhombic geometry and along the applied load direction for the square geometry.

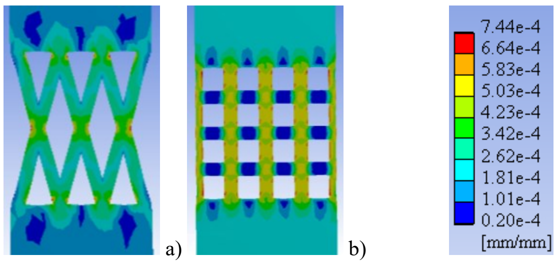

Fig.16.Longitudinal strain (in mm/mm) by means of FE modelling for a) rhombic and b) square weft trabecular specimen.

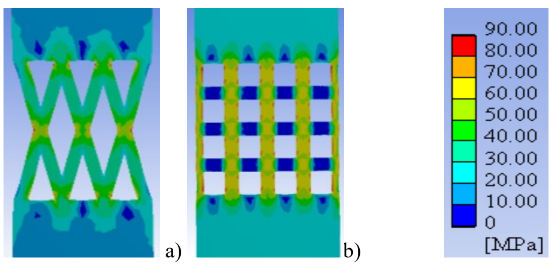

Fig.17.Von Mises equivalent stress (in MPa) by means of FE modelling for a) rhombic and (b) square weft trabecular specimen.

E. Modal analysis results

Modal analysis was performed exploiting PolyMAX algorithm [16][17] for modal parameters extraction. Fig. 18 reports the comparison between the Sum FRFs (average FRF over spatial domain) estimated on the tests with the acoustic source placed at the tip (green curve) and at the constraint (red curve).

As expected, considering the quite high mobility of the structure, the excitation at the constraint take advantage from the higher mechanical impedance, and it is much more effective, with the ability to highlight more resonance peaks. Fig. 19 shows some mode shapes obtained in this excitation condition.

Fig. 20 shows the comparison between the Sum FRF and the Power Spectral Density (PSD) of the excitation signal supplied to the piezoelectric transducer for the 10-102 kHz excitation range. The excitation decay over 70 kHz is a proof that this excitation range should not be considered in the analysis.

The lower frequency range (around 10 kHz) seems to be still affected by global modes. This is proved if looking at mode shapes calculated in this range. Fig. 21 show an example in which the presence of global modes (showing up as "rigid body modes" for the trabecular cell) prevents a correct assessment of trabeculae dynamic behavior.

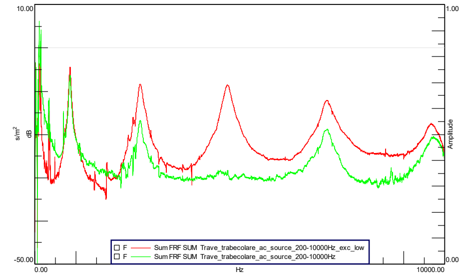

Fig.18.FRF comparison between constraint (red) and tip (green) excitation

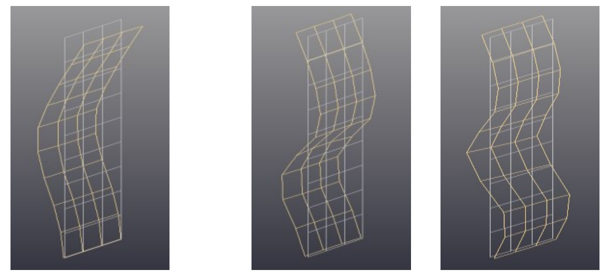

2^ bending (848.3 Hz) | 3^ bending (2566.0 Hz) | 4^ bending (4696.7 Hz)

Fig. 19. Mode shapes with acoustic excitation

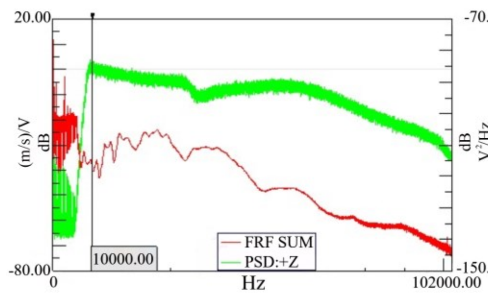

Fig.20.Piezo-based excitation test: Sum FRF Vs Reference PSD for the 10-102 kHz frequency range excitation

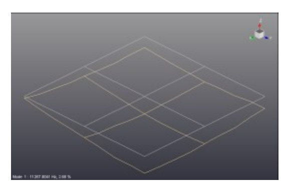

Fig.21.Trabeculae Mode shape at 11 kHz: global modes mask the local dynamic behavior of the lattice structure

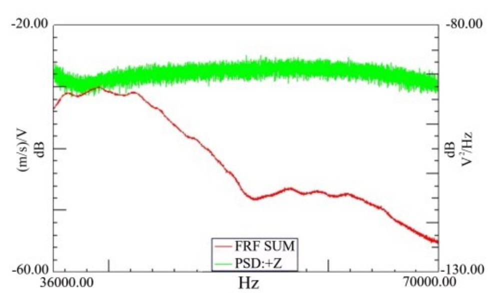

Fig.22.Piezo-based excitation test: Sum FRF Vs Reference PSD for the 35-70 kHz frequency range excitation

Fig. 22 shows the Sum FRF and the PSD of the amplifier signal for the second frequency range investigated, i.e. 35-70 kHz. The mode shapes reported in Fig. 23 appear now more evident, showing interesting local effects. Unfortunately, it was not possible to increase the spatial density of the measurement points, in order to avoid the risk of spatial aliasing, which is likely to happen in higher frequency maps.

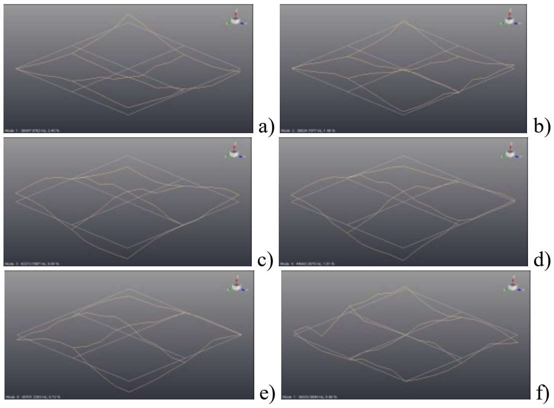

Fig.23.Trabeculae Mode shapes at 36.0, 38.6, 42.2, 44.6, 50.7 and 56.5 kHz obtained with piezoelectric actuator

IV. Conclusions

Lattice structures represent interesting structures for many engineering applications. When it comes to these structures, additive manufacturing is the only technological solution for their manufacturing, given the presence of complex pattern of voids as well as thin and columnar elements (trabeculae) highly interwoven. The development of full-field experimental techniques and specific test protocols, to evaluate morphology, stress-strain state and modal behavior, is an actual issue and of great interest for practical application of this new class of structures. Some preliminary results obtained on specimens with elementary trabecular morphology using a multi-instrument and multi-competence approach were presented in this paper. This approach made it possible to analyze different aspects ranging from dimensional accuracy and surface morphology to the structural response in terms of stress-strain distribution and modal behavior. Future work will be addressed to extend the characterization to 3D analysis as well as to apply it to real components.

V. Acknowledgement

This work was supported by the Ministry of Education, University and Research in Italy (MIUR) under the Research Project of National Interest (PRIN2015) “Experimental techniques for the characterization of the effective performances of trabecular morphology structures realized in additive manufacturing”.

VI. References

[1] Minh-Son Pham, Chen Liu, Iain Todd, Jedsada Lertthanasarn, Damage-tolerant architected materials inspired by crystal microstructure, Nature, Volume 565, 305–311, 2019

[2] F. Calignano et al., "Overview on Additive Manufacturing Technologies," in Proceedings of the IEEE, vol. 105, no. 4, pp. 593-612, April 2017. doi: 10.1109/JPROC.2016.2625098

[3] S. G. Keaveney and D. P. Dowling, "Application of additive manufacturing in design & manufacturing engineering education," 2018 2nd International Symposium on Small-scale Intelligent Manufacturing Systems (SIMS), Cavan, 2018, pp. 1-6. doi: 10.1109/SIMS.2018.8355289

[4] F. G. Sisca, C. M. Angioletti, M. Taisch and J. A. Colwill, "Additive manufacturing as a strategic tool for industrial competition," 2016 IEEE 2nd International Forum on Research and Technologies for Society and Industry Leveraging a better tomorrow (RTSI), Bologna, 2016, pp. 1-7. doi: 10.1109/RTSI.2016.7740609

[5] L. Leonardi, F. Piro, V. Pannaioli, E. Bellezza, R. Marsili, G. Angeli, et al., “Additive manufacturing and advanced testing techniques applied to bone reconstructive sciences in animals and humans”, in Easy Chair SISVET 2015, Perugia, Italy, 15-17 June 2015.

[6] A. Sutradhar, J. Park, D. Carrau and M. J. Miller, “Experimental validation of 3D printed patient-specific implants using digital image correlation and finite element analysis”, Comput. Biol. Med., vol. 52, pp, 8-17, 2014.

[7] L. S. Dimas and M. J. Buehler, “Modeling and additive manufacturing of bio-inspired composites with tunable fracture mechanical properties,” Soft Matter, vol. 10, pp. 4436-4442, 2014.

[8] F. Li, J. Li, G. Xu, G. Liu, H. Kou and L. Zhou, “Fabrication, pore structure and compressive behavior of anisotropic porous titanium for human trabecular bone implant applications”, J. Mech. Behav. Biomed. Mater., vol. 46, pp. 104-114, 2015.

[9] F. Brenne, T. Niendorf and H. J. Maier, “Additively manufactured cellular structures: Impact of microstructure and local strains on the monotonic and cyclic behavior under uniaxial and bending load”, J. Mater. Process. Technol., vol. 213, pp. 1558-1564, 2013.

[10] J. Karlsson, T. Sjögren, A. Snis, H. Engqvist and J. Lausmaa, “Digital image correlation analysis of local strain fields on Ti6Al4V manufactured by electron beam melting”, Mater. Sci. Eng. A, vol. 618, 456-461, 2014.

[11] A. S. Wu, D. W. Brown, M. Kumar, G. F. Gallegos and W. E. King, “An Experimental Investigation into Additive Manufacturing-Induced Residual Stresses in 316L Stainless Steel”, Metall. Mater. Trans. Phys. Metall. Mater. Sci., vol. 45, pp. 6260-6270, 2014.

[12] Z. J. Wally, W. van Grunsven, F. Claeyssens, R. Goodall and G.C. Reilly, “Porous Titanium for Dental Implant Applications”, Metals, vol. 5, pp. 1902-1920, 2015.

[13] G. Allevi, M. Cibeca, R. Fioretti, R. Marsili, R. Montanini, G. Rossi, “Qualification of additively manufactured aerospace brackets: A comparison between thermoelastic stress analysis and theoretical results”, Measurement, vol. 126, pp. 252-258, 2018.

[14] C. Bailey, S. Stoyanov, T. Tilford and G. Tourloukis, "Multi-physics models and condition-based monitoring for 3D-Printing of electronic packages," 2017 18th International Conference on Thermal, Mechanical and Multi-Physics Simulation and Experiments in Microelectronics and Microsystems (EuroSimE), Dresden, 2017, pp. 1-8. doi: 10.1109/EuroSimE.2017.7926286

[15] G. Allevi et al., “Qualification of additive manufactured trabecular structures using a multi-instrumental approach”, 2019, Proceedings of IEEE I²MTC 2019, Auckland, New Zeland.

[16] P. Guillaume, P. Verboven, S. Vanlanduit, H. Van der Auweraer and B. Peeters, “A poly-reference implementation of the least-squares complexfrequency-domain estimator”, Proceedings of IMAC 21, the International Modal Analysis Conference, 2003, Kissimmee (FL), USA.

[17] B. Peeters, H. Van der Auweraer, P. Guillaume, and J. Leuridan, “The PolyMAX Frequency-Domain Method: A New Standard for Modal Parameter Estimation?”, Shock and Vibration, vol. 11, no. 3-4, pp. 395-409, 2004.

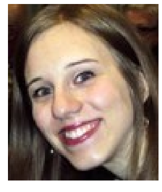

G. Allevi received the Master’s Degree in Mechanical Engineering from Università Politecnica delle Marche, Ancona, Italy, in February 2016. She is achieving the Ph.D. degree in “Mechanical Measurement for Engineering and Space” at the Centre of Space Activities and Studies “G. Colombo” of University of Padova, Italy. Her work focuses on Non-Contact measurement techniques for Structural Health Monitoring of aerospace materials, like composites or Additively Manufactured components.

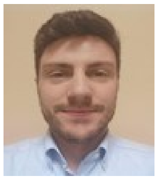

L. Capponi received the Bachelor and the Master of Science degrees in mechanical engineering from the University of Perugia in 2014 and 2017. He is now Ph.D. student in mechanical measurements for engineering and space at the University of Padova at the "G. Colombo" CISAS, Padova, Italy. His current research interests include numerical and experimental analysis, stress and strain measurements, thermoelasticity, vibrational fatigue, topology optimization and additive manufacturing.

P. Castellini received the PhD degree in 1996 at University of Padova, Italy.
In 1997, he joined the Mechanical Department of Ancona, as an researcher and in 2011 become Associate Professor at the Department of Industrial Engineering and Mathematical Sciences at the Polytechnic University of Marche, where he teaches Mechanical and Thermal Measurements and Testing. He has more than 24 years activity in the development of instrumentation for mechanical measurements.

P. Chiariotti received the M.S. degree in Mechanical Engineering in 2007 and the Ph.D. degree in Mechanical Engineering and Management from Università Politecnica delle Marche – UNIVPM (Italy) in 2011. He currently holds a researcher position in Mechanical and Thermal Measurements at the Faculty of Engineering of UNIVPM. Member of IEEE, for which he chairs the technical committee on Vibration and acoustic sensors of the IEEE Italy Sensor chapter, and SEM (Society for Experimental Mechanics).

F. Docchio received his M.S. Degree in 1976. He worked at the Centro di Elettronica Quantistica of Italy between 1978 and 1987, where he carried out research concerning laser development and applications in industry and bio-medicine. In 1987 he joined the Dipartimento di Elettronica per l'Automazione of the University of Brescia. He is now Full Professor of Electrical Measurements at the Department of Mechanical and Industrial Engineering of the University of Brescia. He is a member of the Laboratory of Vision Systems for Mechatronics. He is currently Fellow of the European Optical Society.

F. Freni is a Materials Engineer, graduated at University of Messina in 2009. In the same institution, in 2013 he completed the Ph.D. program in Mechanical and Thermal Measurements, focusing his research on infrared thermography and NDT&E. He is currently collaborating with the University of Messina on researches involving optical measurement techniques, including TSA and digital image correlation, measurement uncertainty estimation and image post-processing.

R. Marsili is Researcher of Mechanical Measurements at University of Perugia. He is graduated in Mechanical Engineering and he obtained the PhD degree from University of Padova studying piezoelectric films. His area of interest regards diagnostics of mechanical systems, thermoelastic stress analysis, development of optical sensors for distance and shape measurements, study of methodologies for the measurement of contact pressure between two surfaces.

M. Martarelli received the M.S. degree in Mechanical Engineering from Università Politecnica delle Marche (UNIVPM), Ancona, in 1997. She received the Ph.D. degree in Structural Mechanics from Imperial College, London, in 2001. She is Associated Professor at UnivPM with 20 years of experience in Mechanical and Thermal Measurement. Her research interests focus on non-contact measurement sensors applied to Non-Destructive Diagnostics and vibro-acoustics for systems performance assessment.

R. Montanini is full professor of Mechanical and Thermal Measurements at the University of Messina. He received the M.Eng in Mechanical Engineering and the Ph.D. at the Politecnico di Torino. In 2001 he founded the Laboratory of Mechanical and Thermal Measurements and in 2016 the Laboratory of Non-destructive Evaluation and Structural Health Monitoring. His main research interests are in the field of active infrared thermography, fiber optic sensing, structural diagnostics and defect detection.

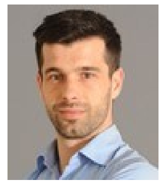

S. Pasinetti received the M.S. degree (with honors) in Automation Engineering from University of Brescia, Brescia, Italy, in 2011, with a thesis concerning the control of mechanical actuators with SEMG signals. He received the Ph. D. degree in applied mechanics from University of Brescia, Brescia, Italy, in 2015. Since January 2015, he has been a research fellow for the Laboratory of Vision Systems for Mechatronics (Vis4Mechs) in the Department of Mechanical and Industrial Engineering at University of Brescia, Italy.

A. Quattrocchi is currently Researcher Fellow in Mechanical and Thermal Measurements at the University of Messina, Italy. He received his B.Eng., M.Eng. and Ph.D. degrees from the University of Messina in 2011, 2013 and 2017, respectively. He was Visiting Scholar at University of California, San Diego in 2016. His main research topics are focused on active infrared thermography, piezoelectric smart sensors, defect detection, vibro-acoustics and electro-mechanical materials.

R. Rossetti was graduate in Mechanical Engineering at the UNIVPM, then carried out research at the same university in the experimental verification of high damping structures made by trabecular construction in additive manufacturing. During this activity he worked on national Additive Manufacturing and European projects on the creation of multi-agent cyber-physical systems capable of supporting production systems in Zero Defect Manufacturing.

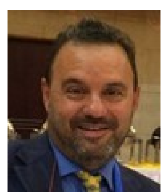

G. Rossi is professor of "Mechanical and Thermal Measurements" at University of Perugia. At University of Padova he teaches also "Measurement techniques for Industrial diagnostics" in the PhD school in Space Sciences, Technologies and measurement techniques. President of Tucep association involving 12 italian Universities, Industries and public institutions with the mission of technology transfer, Erasmus programs, training and research. Author of more than 130 scientific publications..

G. Sansoni received her degree in Electronic Engineering at the Politecnico of Milan, Italy, in 1984. In 1985 she joined the University of Brescia, Italy. She is now Full Professor of Electrical Measurements at the Department of Mechanical and Industrial Engineering of the University of Brescia. Her main research interests are in the 3D vision area for the acquisition of free-form surfaces. She is currently the head of the Laboratory of Visions Systems for Mechatronics at University of Brescia, Brescia, Italy.

E.P. Tomasini received the M.S. degree in mechanical engineering from the Università La Sapienza, Roma, in 1972. He was professor of Mechanical and Thermal Measurement at University of L'Aquila, AQ, Italy, in 1975-76. He is Full Professor since 1989 at UNIVPM. He is the author of more than 150 publications on books, journals and national and international conference proceedings. His research interests include non-contact measurements in application fields ranging from mechanics and fluid dynamics.